Numerical study of aerodynamics for three wind turbines with two different layouts

Xinze Duan, Yong Ai and Decheng Wan*

Collaborative Innovation Center for Advanced Ship and Deep-Sea Exploration, State Key Laboratory of Ocean Engineering, School of Naval Architecture, Ocean and Civil Engineering, Shanghai Jiao Tong University, Shanghai 200240, China

Abstract: Wind energy is one of the most promising non-polluting renewable energy sources. How to efficiently exploit and utilize the wind energy resources and reasonably reduce the wind farm area will become an important and noteworthy research topic. The optimal arrangement of wind turbine for the wind farm is the key link in the planning and designing stage, the layout of the wind farm will directly affect the power generating capacity and the economic efficiency of the wind farm. In order to rationally arrange the wind turbines, minimize the mutual interference in the wake, and improve the efficiency of the whole wind farm, in this paper, the complex phenomenon of wake interaction among three wind turbines is studied based on the actuator line model (ALM) combined with CFD technique, and the LES turbulence model is solved in the simulations conducted in the OpenFOAM. In this paper, aerodynamics for three wind turbines with two different layouts have been studied, one is the in line model, and the other is the offset model, meanwhile maintaining the longitudinal spacing of the three wind turbines consistent. Numerical simulations are conducted to predict the performance, the wake development and the wake interaction under the two different layouts. From the study, it is concluded that the aerodynamic power output of the downstream wind turbine exits a significant decrease relative to the upstream wind turbine. Furthermore, compared with the aerodynamic loads of turbines between the two different layouts, it shows that the mean aerodynamic power output of the downstream wind turbine with the offset layout which is higher than the in line model, but the effect of the partial impingement of the wake developed by the upstream turbine also creates more damaging fatigue loads. Moreover, the complex wake interaction will impact the aerodynamic loads and the wake development of wind turbines seriously.

Keywords: wind farm; actuator line model; CFD; wake interaction; aerodynamic power;

Article ID: 1671-9433(2016)01-0000-00

1 Introduction

With depletion of traditional fossil fuels, environmental pollution and global warming becoming more and more serious, it is urgent for us to develop new clean energy (Morato *et al.*, 2001). Wind energy, as a kind of clean and renewable energy, has become the research hotspots of the energy development in the past ten years because of plentiful resources reserves, wide distribution and no pollution. Wind turbines are only used to extract the renewable energy from the wind which have showed the rapid increase in both the total number of wind turbines installed and the maximum wind power capacity with the rapid development of wind energy technology (Jeon *et al.*, 2013). Wind farms composed of large capacity wind turbines will become the future trend of development of wind energy (Abderrazzaq and Hahn., 2006). Since the broader application of wind energy, the layout design of the wind farm is becoming significant (Chio *et al.*, 2014). The optimal arrangement of wind turbine for the wind farm is the key link in the planning and designing stage, the layout of the wind farm will directly affect the power generating capacity and the economic efficiency of the wind farm (Kusiak and Song., 2010). Among several wind farm layout design factors, the arrangements of the wind turbines which have a great influence on the aerodynamic load, wind velocity deficit, wake vortex structure and even fatigue loads. Therefore, it is necessary to thoroughly research in this regard.

In order to study the complex phenomenon existing in wind farms, some scholars have tried to use wind tunnel experiment to study the wake vortex structure of a single turbine and the wake interaction of multiple wind turbines. Vermeer *et al.*, (2003) researched the near wake and far wake for a single turbine and wind farms with the uniform, steady and parallel flow conditions by using wind tunnel experiment, meanwhile the experimental and numerical results were compared with each other. Krogstad and Eriksen., (2013) presented an experimental investigation of the aerodynamic load, wind velocity defect and turbulent kinetic energy distribution in the wake of the multiple wind turbines, meanwhile the results were compared with a wide range of methods. Even though the experimental method can provide useful information about some main features of the wake structure, the defects of such studies is that low Reynolds number and scale effects can't be eliminated relative to the full scale (Troldborg *et al.*, 2011). Obviously, it is unrealistic to use the experimental method to study the wake interaction for wind farms in full scale because of the high cost required and the long time period involved. Chio *et al.*, (2013, 2014) have done a study focused on comparing the effect of the different mutual distance between the wind turbines for the wind farms composed with two and three wind turbines

***Corresponding author Email: dcwan@sjtu.edu.cn**

which both have the linear layout called tandem type with the CFD method, and the RANS equations with k-ω SST turbulence model were solved in the simulations. The aerodynamic power output of the 2 MW class wind turbine has been studied and analyzed by using a full wind turbine model considering the influence of the hub and tower, which may take a long time to get final answers because of too large mesh numbers. A mixed method named actuator line model combined with CFD technique was developed by Sørensen and Shen (2002). Some researchers have done lots of work about the wind farm simulation using actuator line model. Troldborg *et al.*, (2011) presented numerical simulations to analyze the phenomenon of wake interaction between two wind turbines using actuator line method and full unsteady Navier-Stokes computations coupled with EllipSys3D software (Michelsen, 1994; Sørensen, 1995). Various inflow conditions were taken into account, the varying inter-turbine distances between the two turbines in both tandem and offset configurations with the different degrees of ambient turbulence intensity were considered. A high-fidelity tool SOWFA (*Simulator for Wind Farm Applications*) (Churchfield and Lee, 2013), which is a LES framework coupled with FAST (*Fatigue, Aerodynamics, Structures, Turbulence*) (Jonkman, 2010), was used to analysis offshore wind turbine and wind farm based on that method. Churchfield *et al.*, (2012) have done a large-eddy simulation of the Lillgrund wind plant which contains 48 multi-megawatt turbines, and turbines were modeled using actuator line representation. This work presented aerodynamics and power-production results of the large wind farm, and wake effects among multiple wind turbines were discussed.

In this study, the complex wake interactions among three wind turbines with the linear and offset two different layouts are analyzed using a technique that combines an actuator line model and large eddy simulations (LES). The purpose of this work is to get some detailed information about the wake interaction and to deeper study the effect of the upstream turbine on the aero-power and aero-thrust of the downstream turbines.

2 NUMERICAL METHODS

2.1 Actuator Line Model

The actuator line model (ALM) was firstly developed by Sørensen and Shen (1999). The basic thought of this method is to replace the blades of the wind turbine with the lines which body forces are distributed radially. So the main advantage is that it is not required to build the actual blades model, the much fewer grid points are needed. Moreover, the lift force and drag force of each section can be calculated as:

$$L=\frac{1}{2}C_l(\alpha)\rho U_{rel}^2 cdr \quad (1)$$

$$D=\frac{1}{2}C_d(\alpha)\rho U_{rel}^2 cdr \quad (2)$$

Where, C_l and C_d are the lift and drag coefficient, respectively. α is the attack angle, c is the chord length, U_{rel} is the local velocity relative to the rotating blade of each section.

In Fig. 1 we can know that the local velocity relative to the rotating blade can be expressed as:

$$U_{rel}=\sqrt{U_z^2+(\Omega r-U_\theta)^2} \quad (3)$$

There, the U_z and U_θ are the axial velocity and tangential velocity, respectively. The Ω is the rotational velocity of rotors.

The body force f can be expressed as:

$$f=(L,D)=\frac{1}{2}\rho U_{rel}^2 c\left(C_l\vec{e_L}+C_d\vec{e_D}\right) \quad (4)$$

The aerodynamic blade force that cannot be directly applied to the flow field, it need to be distributed smoothly on the flow field volume in order to avoid singular behavior. In practice, a 3D Gaussian function is made to smooth the force over the blade by taking the convolution of the force with a regularization kernel.

$$f_\varepsilon=f\otimes\eta_\varepsilon \quad (5)$$

$$\eta_\varepsilon(d)=\frac{1}{\varepsilon^2\pi^{3/2}}\exp\left[-\left(\frac{d}{\varepsilon}\right)^2\right] \quad (6)$$

Here, d is distance between cell-centered grid points and the actuator line point, and ε is parameter that serves to control the width of Gaussian and to adjust the concentration of the regularized loads.

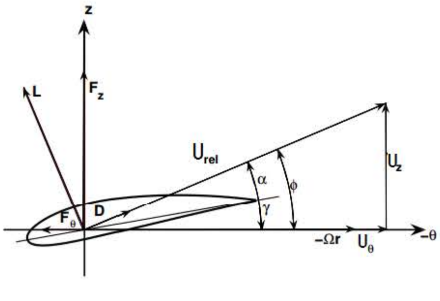

Fig. 1 Cross-sectional aero foil element (Sørensen and Shen, 2002)

2.2 Governing Equation

In LES model, the instantaneous velocity field U_i is divided into two parts: a large scale local averaged part $\overline{u}_i$ which is directly calculated, a sub-grid scale part $\overline{u}_i'$ which should be modeled using Sub-Grid Scale (SGS) models. The Navier-Stokes equations of incompressible flow are spatially filtered to arrive at the resolved-scale can be expressed as follows:

$$\frac{\partial\overline{u}_i}{\partial x_i}=0 \quad (7)$$

$$\frac{\partial(\rho\bar{u}_i)}{\partial t}+\frac{\partial\left(\rho\overline{u_iu_j}\right)}{\partial x_j}=-\frac{\partial\bar{p}}{\partial x_i}+\frac{\partial}{\partial x_j}\left[\mu\left(\frac{\partial\bar{u}_i}{\partial x_j}+\frac{\partial\bar{u}_j}{\partial x_i}\right)\right]+f_i^T \quad (8)$$

Where, f_i^T denotes the body force, which represents the loading on the blades exerted by the actuator line turbine model. Here the subgrid scale Reynolds stress τ_{ij} is introduced, and defined as:

$$\tau_{ij}=-\rho\left(\overline{u_iu_j}-\bar{u}_i\bar{u}_j\right) \quad (9)$$

The well-known Smargorinsky model is chosen as Sub-grid stress model for turbulence closure:

$$\tau_{ij}-\frac{1}{3}\tau_{kk}\delta_{ij}=2\mu_t\bar{S}_{ij} \quad (10)$$

Where μ_t the eddy viscosity, $\bar{S}_{ij}$ the strain rate of the large scale and δ_{ij} is the Kronecker delta. The form of the subgrid scale eddy viscosity is:

$$\mu_t=C_S^2\rho\Delta^2\left|\bar{S}\right| \quad (11)$$

Where $\left|\bar{S}\right|=\sqrt{2\bar{S}_{ij}\bar{S}_{ij}}$ and the stress rate is defined as:

$$\bar{S}_{ij}=\frac{1}{2}\left(\frac{\partial\bar{u}_i}{\partial x_j}+\frac{\partial\bar{u}_j}{\partial x_i}\right) \quad (12)$$

and Δ denotes the filter length scale, $\Delta=\left(\Delta_x\Delta_y\Delta_z\right)^{1/3}$.

3 SIMULATION SETUP

The NREL 5MW baseline wind turbines were developed by The U.S. Department of Energy's National renewable energy laboratory, the blade airfoils of them consist of Cylinder, DU and NACA64. In addition, the rotational direction of the rotor is clockwise and the rotational phase of each wind turbine is synchronized. Table 1 gives some specification of NREL 5MW baseline wind turbine used in this present study.

Table 1 Parameters of NREL-5MW turbine

Name	Parameter
Rating	5 MW
Rotor Orientation	Upwind
Number of blades	3
Rotor Diameter, Hub Diameter	126 m, 3 m
Hub Height	90 m
Cut-in, Rating, Cut-out	3 m/s, 11.4 m/s, 25 m/s
Cut-in, Rating Rotor Speed	6.9 rpm, 12.1 rpm

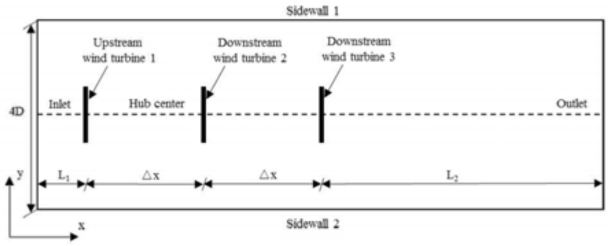

(a) The in-line model

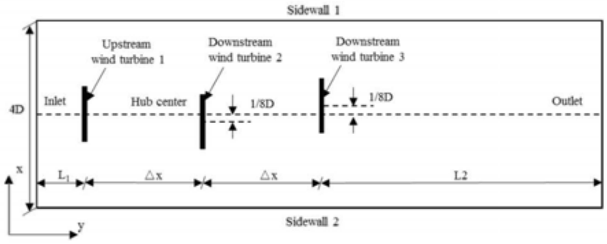

(b) The offset model

Fig. 2 The different arrangements of wind farms

The wind farms contain three wind turbines with two different layouts are studied in this paper, one is the in-line model, and the other is the offset model, meanwhile maintaining the longitudinal spacing of the three wind turbines consistent. There is a crosswind offset of 1/8 rotor diameter between the upstream turbine and the both downstream turbines respectively in the offset model. The detail arrangements are showed in Fig. 2. All distances are based on the rotor diameter D equal to 126m. The width and height of the wind farm flow field are both kept at 4D. The distance L1 from the inlet to the upstream wind turbine and the distance L2 from the outlet to the latter downstream wind turbine are kept at 1D and 6D, respectively. In different configurations, the distance Δx which is the distance between the two adjacent turbines remains unchanged, equal to 2.5D. The downstream wind turbines with the in-line and offset configurations are both placed in the strong wake region of upstream wind turbine, which aims to observe the effect of the layouts on the aerodynamics for the wind farms obviously.

The grid extension regions for the whole numerical computation are differently imposed in order to fully resolve the strong gradients in the vicinity of the actuator lines and carefully observe significant meandering of the wake. The both cases use the same mesh system. The first part is the outer mesh which is an initial mesh part for the whole flow field; from the Fig.3 (b), it can be figured out that the range of the second part which has one level refinement based on the initial mesh is from 0D to the end in the flow direction and from -0.8D to 0.8D in height and width direction. There is the third part whose refine level is two, the length and the width of this part is the same as the second part, while the distance in the height direction is from the -0.6D to 0.6D. The aim of the mesh refinement is to capture the near wake characteristics for each wind turbine

(a) Grid in lengthwise section (b) Grid in cross section

Fig. 3 The grid in lengthwise section and cross section

The uniform inflow model is used in both simulation cases, ignoring wind shear effect. Thus, the enforced conditions are as follow: the free-stream flow whose velocity is equal to the rated speed 11.4 m/s, the rotation speed of the blades of all wind turbines in the wind farm is the rating speed, 12.1rpm. Furthermore， we do not model the effect of the nacelle and tower to decelerate the fluid. In this study, the rated wind speed of 11.4m/s is applied to the inlet defined in Fig. 2. A relative pressure of 0 Pa based on the atmospheric pressure is chosen for outlet boundary. Free-slip condition is applied to the top boundary, which means there is no wind speed gradient vertically and no flow across the top surface. The no-slip condition is applied to the bottom boundary. Meanwhile, the symmetry boundary conditions are applied to the sidewall 1 and sidewall 2.

The duration of the whole computation is about 200 seconds to ensure that full development of the wake of all turbines in the wind farms, especially the last turbine which id seriously affected by the upstream turbine. The computational time step is given to 0.005s to avoid the numerical divergence and more accurate transient performance of the aerodynamics and numerical data could be obtained. Meanwhile, the parameter ε existed in Eq. 6 and named Gaussian width parameter, adjusts the concentration degree of the body force in the Gauss distribution. The smaller the value of ε, the more concentrated distribution of the volume force. So this value of ε is roughly the minimum at which the force is smoothed enough to avoid spurious oscillations in the resulting velocity field using a central spatial discretization scheme (Churchfield, 2012). In this study, the parameter ε is kept to equal to twice the local grid size around blades (Martínez *et al.*, 2012).

4 RESULT AND DISSCUSION

In this present study, aerodynamics and the complex phenomenon of wake interaction among three wind turbines with two different layouts is studied based on the actuator line model (ALM) combined with CFD technique.

4.1 Aerodynamic loads prediction

Due to the impulsive start-up of the rotor at the beginning of each simulation, both the upstream wind turbine and downstream turbines undergo a transient overshoot. In order to avoid the effect of the initial transient loads and to consider the full development of the wake of the upstream turbine, the time history curves of aerodynamic loads from 150 seconds to 200 seconds are shown in Fig. 4 and 5. Fig. 4 shows the time-history of aerodynamic power while Fig. 5 shows the time-history of aerodynamic thrust.

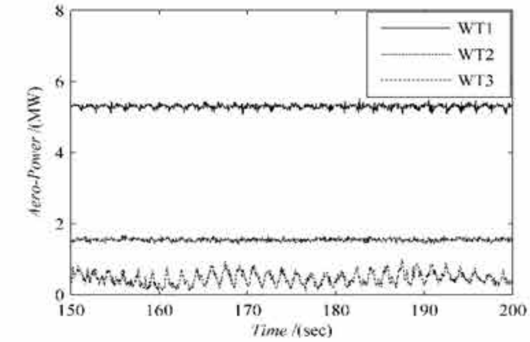

(a) The in-line model

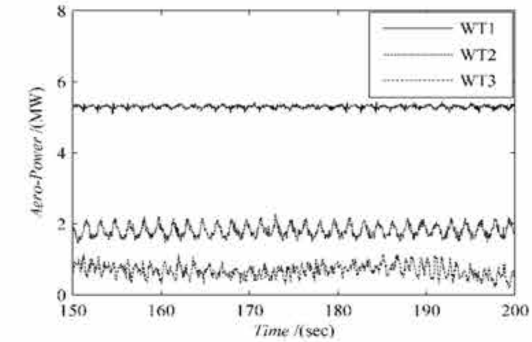

(b) The offset model

Fig. 4 Time history curves of aerodynamic power output of upstream and downstream wind turbines with the different layouts.

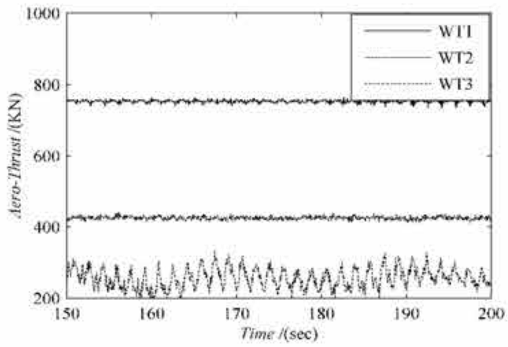

(a) The in-line model

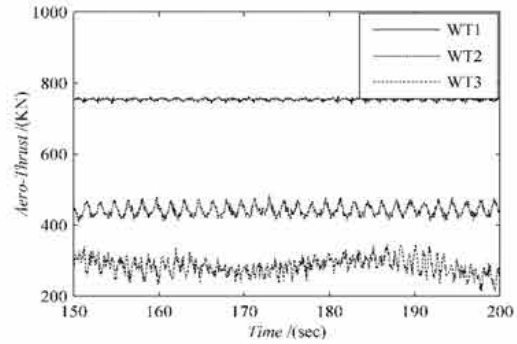

(b) The offset model

Fig. 5 Time history curves of aerodynamic thrust of upstream and downstream wind turbines with the different layouts.

From the pictures, it can be figured out that there is a strong interaction between the upstream and downstream wind turbines in the wind farm whether the configuration is the in-line or the offset. The aerodynamic power outputs of upstream wind turbine in the different cases nearly keep in the similar value slightly greater than the rated power, because the incident wind speed is almost unchanged to the upstream wind turbine, and the downstream turbines have a little impact on the upstream turbine. Conversely, the obvious wind speed deficit compared to the upstream wind speed leads to the serious decrease in the aerodynamic power output and aerodynamic thrust of downstream wind turbines due to the presence of upstream wind turbine. The comparisons of the mean aerodynamic power and thrust among all the turbines with the different layouts are present in Fig. 6. From Fig. 6, it is obvious that the aerodynamic power and thrust of downstream wind turbines are changed because of a strong interaction between the upstream and downstream wind turbines in the wind farms which are designed as the typical linear layout and the offset layout. Table 2 lists the aerodynamic power output of wind turbines and power output ratio, which can be defined as:

$$\textit{power output ratio}=\frac{\textit{power out of downstream wind turbine}}{\textit{power out of upstream wind turbine}} \quad (13)$$

Table 2 Aerodynamic power output of wind turbines and power output ratio

Layouts	WT ID	Power (MW)	Power ratio WT2/WT1	Power ratio WT3/WT1
In-line	WT1	5.820	26.60%	7.92%
	WT2	1.548		
	WT3	0.461		
Offset	WT1	5.823	31.05%	11.47%
	WT2	1.808		
	WT3	0.668		

Compared with the aerodynamic loads of turbines between the two different layouts, it can be easily concluded that the mean aerodynamic power and thrust of wind turbines that is offset in the crosswind direction by 1/8 rotor diameter is greater than the mean aerodynamic power and thrust of the same turbines when the arrangement with no crosswind offset, expect the first turbine at the upstream. Although the mean aerodynamic power and thrust of downstream turbines with the offset layout increase significantly, it is accompanied by the unsteadiness in the performance of the downstream turbines. The reason of the aerodynamic loads increasing and the unsteadiness occurs is that the wake developed by the upstream turbine impinges partially on the downstream rotor disc. The effect of the partial impingement of the wake developed by the upstream turbine also creates more damaging fatigue loads as turbine blades periodically pass into and out of the partial wakes.

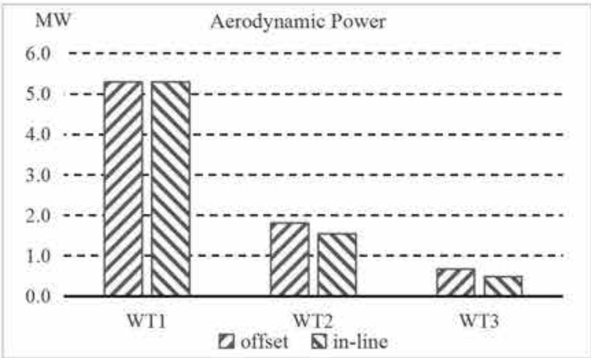

(a) The aerodynamic power

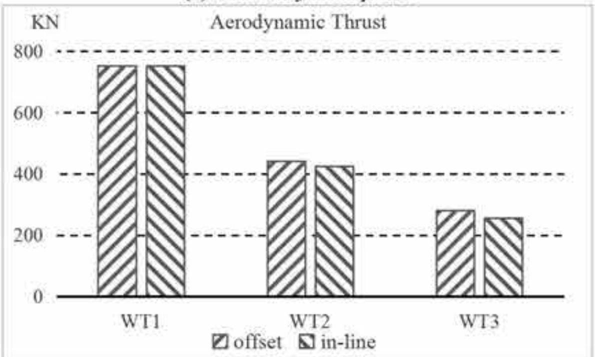

(b) The aerodynamic thrust

Fig. 6 Comparison of the mean aerodynamic power and thrust among all the turbines with the different layouts.

In the Fig. 4 and 5, the most noticeable feature of these time history curves of aerodynamic loads, aside from the difference in loads levels, is that there is obvious oscillation in the loads curves of the downstream wind turbines. The loads curves of the wind turbine in the middle with the offset layout have a periodic variation that the frequency of oscillation equals to three times the rotor rotation frequency on these three-bladed turbines roughly while the loads of the same wind turbine with the in-line model maintain a steady state basically. The reason of this interesting phenomenon may be that the middle turbine in the offset model is affected by the partial impingement of the wake developed by the upstream turbine. Furthermore, the phenomenon of the periodic variation also exists in the last turbine of the wind farms which is influenced by the wake of both upstream turbines, so there is no doubt that the inflow condition of the last turbine is very complex. Due to the effect of the asymmetry wake in the offset layout, the oscillation period of offset model is less than the in-line model. From the analysis and research, it can be concluded that when the configuration of the wind farm is the offset in the crosswind direction, the asymmetry interaction can increase the aerodynamic power output of the downstream wind turbines, but also can create more damaging fatigue loads and reduce the life of the wind turbines.

4.2 Wake Characteristics

Fig. 7 shows contours of instantaneous streamwise velocity in horizontal plane through the center of wind turbine rotor for the two different layouts, respectively. These figures are meaningful to understand overall wake flow regions and distinguish the difference for the wake interaction of the in-line and offset configuration. It can be clearly concluded that there are obvious changes of wind speed after the wind passes through the turbines.

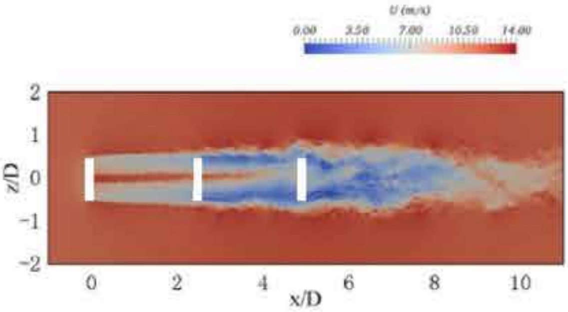

(a) The in-line model

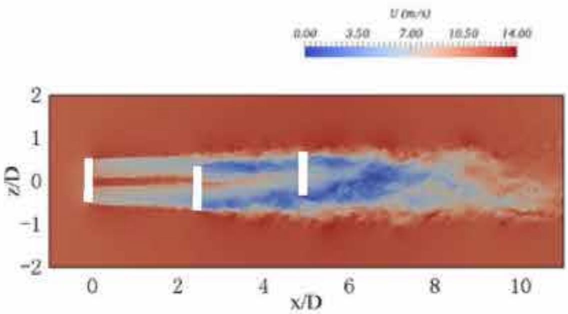

(b) The offset model

Fig. 7 Wind speed contour at hub height in axial direction.

From Fig. 7, it is easy to observe the significant meandering of the wakes, especially the downstream turbines in the both layouts or further downstream. Meanwhile, there is a higher speed region of flow near the center of the rotor. The reason for this phenomenon is that the effect of the hub, nacelle and tower are not considered in present simulation. It can also imply that the influence of upstream wind turbine on wake is significant, so there is still strong wake interference which is the main reason that causes the serious decrease in velocity of wake flow.

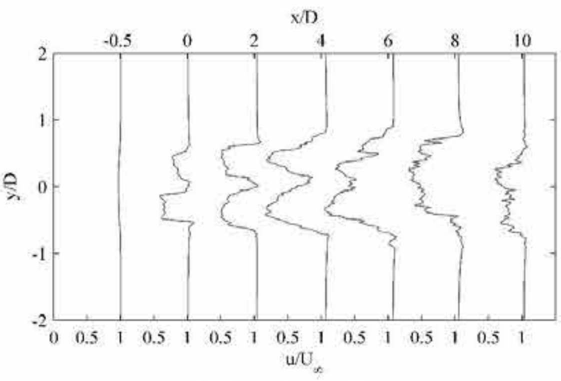

(a) The in-line model

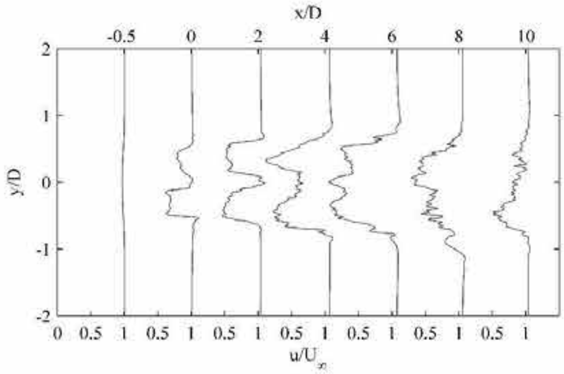

(b) The offset model

Fig. 8 Profiles of the streamwise velocity in horizontal plane through the center of wind turbine rotor

The profiles of the streamwise velocity at hub height is shown in Fig. 8 corresponding to the fig. 7 respectively. The sharp decrease of the speed of flow and the phenomenon of the wake expansion can be clearly observed in the both cases. Furthermore, owing to the offset in the crosswind direction, the radius of speed decline is bigger than the in-line wind turbines. Due to considering the instantaneous streamwise velocity, there are many irregular fluctuations in the profiles of the wind speed, the reason for this phenomenon may be the presence of the significant meandering of the wakes. In addition, when the wind passes through the rotor of wind turbine, the axial direction wind speed decrease sharply, then recovered slightly until passing through the rotor of the next wind turbine. As Choi *et al* (2013) pointed out that, in theory, a complete recovery of the downstream wind turbine's power output requires infinite separation distance between wind turbines, it can be believed that there will be strong interaction among the wind turbines in the wind farm.

4.3 Vortex structure

Fig. 9 shows the instantaneous vorticity contours for the wind farms with the both arrangements respectively. It can be clearly seen that the tip vortex periodically shedding from each blade of the upstream wind turbine. With the development vertex, the vortex generated by upstream wind turbine is mixed with the vortex produced by downstream wind turbine, the vortex structure of wind field becomes very complicated. Meanwhile, the radius of the vortex becomes larger than the vortex that just shedding from upstream wind turbine due to the wake expanding effects and the mixed vortex effects. Furthermore, compared with the vortex structure conducted by the two different layouts, although there is a crosswind offset of 1/8 rotor diameter between the upstream turbine and downstream turbines in the offset model, the difference is not obvious because of the significant the wake expanding effects in the both models. From the development of the vortex for the wind turbines, it can clearly figure out that the strong and complex wake interaction phenomenon in the three wind turbines will lead to the speed deficit in the wind farm and severely disturb the aerodynamic power output of the downstream wind turbine.

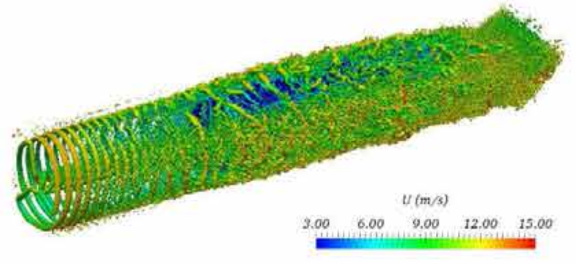

(a) The in-line model

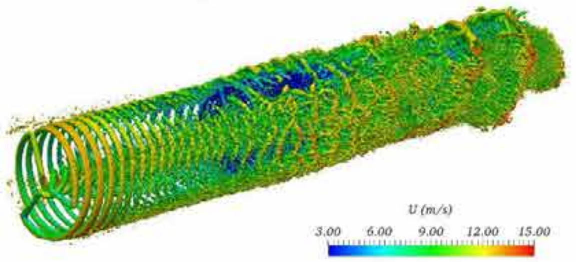

(b) The offset model

Fig. 9 The instantaneous vortex structure for the wind farms

5 Conclusions

In this present study, the aerodynamics and complex phenomenon of wake interaction among three wind turbines in both in-line and offset configurations are analyzed successfully based on the actuator line model combined with CFD technique, and the LES turbulence model is solved in the simulations conducted in the OpenFOAM. From the results and discussion, it can be concluded that the wake interaction between the upstream and downstream wind turbines in the wind farm has a strong effect on the aerodynamics of wind turbine, especially the significant reduction in the local wind speed and aerodynamic power output when the downstream wind turbines subject to the impingement from the wake of the upstream turbine. Contrasting the different layouts, it shows that when the configuration of the wind farm is the offset in the crosswind direction, the blades of the downstream turbines will subject to a highly asymmetric interaction with the wake induced by the upstream turbine. Although the mean aerodynamic power output of the downstream wind turbines with the offset layout increases significantly, the asymmetry interaction will result the significant unsteadiness in the aerodynamic power developed by the downstream turbines and the more damaging fatigue loads on the blades of the turbines, to reduce the lifetime of the wind turbines. Furthermore, the significant meandering of the wakes can be visible, so there are many irregular fluctuations in the instantaneous profiles of the streamwise velocity in horizontal plane through the center of wind turbine rotor for the both different layouts.

In the future work, the impact of the turbulent inflow, inflow speed below rated speed and the effect of the nacelle and tower can be fully considered to study the aerodynamics of wind farms.

6 Acknowledgements

This work is supported by the National Natural Science Foundation of China (51379125, 51490675, 11432009, 51579145), Chang Jiang Scholars Program (T2014099), Shanghai Excellent Academic Leaders Program (17XD1402300), Shanghai Key Laboratory of Marine Engineering (K2015-11), Program for Professor of Special Appointment (Eastern Scholar) at Shanghai Institutions of Higher Learning (2013022), Innovative Special Project of Numerical Tank of Ministry of Industry and Information Technology of China(2016-23/09) and Lloyd's Register Foundation for doctoral student, to which the authors are most grateful.

References

Abderrazzaq MA, Hahn B, 2006. Analysis of the turbine standstill for a grid connected wind farm (case study) [J]. *Renewable Energy*, 31(1):89-104.
DOI: 10.1016/j.renene.2005.02.011

Cheng, P., Wan, D., & Hu, C. (2016, June). Unsteady Aerodynamic Simulations of Floating Offshore Wind Turbines with Overset Grid Technology. *Proc 26th Int Offshore and Polar Eng Conf*, Rhodes, ISOPE, 391-398.

Choi NJ, Sang HN, Jeong JH, et al, 2013. Numerical study on the horizontal axis turbines arrangement in a wind farm: Effect of separation distance on the turbine aerodynamic power output[J]. *Journal of Wind Engineering & Industrial Aerodynamics*, 117(117):11-17.
DOI: 10.1016/j.jweia.2013.04.005

Choi NJ, Nam SH, Jeong JH, Kim, KC, 2014. CFD Study on Aerodynamic Power Output Changes with Inter-Turbine Spacing Variation for a 6 MW Offshore Wind Farm. *Energies*, 7(11), 7483-7498.
DOI: 10.3390/en7117483

Churchfield MJ, Lee S, 2013. *NWTC design codes* (SOWFA).

Churchfield MJ, Lee S, Moriarty PJ, Martinez LA, Leonardi S, Vijayakumar G, et al, 2012. Large-Eddy Simulation of Wind-Plant Aerodynamics: Preprint. *AIAA Aerospace Sciences Meeting*, 537.
DOI: 10.2514/6.2012-537

Jeon SH, Cho YU, Seo MW, et al, 2013. Dynamic response of floating substructure of spar-type offshore wind turbine with catenary mooring cables[J]. *Ocean Engineering*, 72(7):356-364.
DOI: 10.1016/j.oceaneng.2013.07.017

Jonkman J, 2010. NWTC design codes (FAST). *https://nwtc.nrel.gov/FAST*.

Krogstad PÅ, Eriksen PE, 2013. "Blind test" calculations of the performance and wake development for a model wind turbine[J]. *Renewable Energy*, 50:325-333.
DOI: 10.1016/j.renene.2012.06.044

Krogstad PÅ, Sætran L, Adaramola MS, 2015. "Blind Test 3" calculations of the performance and wake development behind two in-line and offset model wind turbines[J]. *Journal of Fluids & Structures*, 52(1):65-80.
DOI: 10.1016/j.jfluidstructs.2014.10.002

Kusiak A, Song Z, 2010. Design of wind farm layout for maximum wind energy capture. *Renewable Energy*, 35(3), 685-694.

DOI: 10.1016/j.renene.2009.08.019

Li, P., Wan, D., & Hu, C. (2016, June). Fully-Coupled Dynamic Response of a Semi-submerged Floating Wind Turbine System in Wind and Waves. *In The 26th International Ocean and Polar Engineering Conference. International Society of Offshore and Polar Engineers.*

Martínez LA, Leonardi S, Churchfield MJ, Moriarty PJ, 2012. "A Comparison of Actuator Disc and Actuator Line Wind Turbine Models and Best Practices for Their Use," *50th AIAA Aerospace Sciences Meeting and Exhibit*, Nashville, TN, Jan. 9–12, AIAA, Washington D.C.
DOI: 10.2514/6.2012-900

Michelsen JA, 1994. *Basis3D-a platform for development of multiblock PDE solvers*. Technical Report AFM 92-05, Department of Fluid Mechanics, Technical University of Denmark.

Michelsen JA, 1994. *Block structured Multigrid solution of 2D and 3D elliptic PDE's*. Technical Report AFM 94-06, Department of Fluid Mechanics, Technical University of Denmark.

Morato A, Sriramula S, Krishnan N, and Nichols J, 2017. Ultimate loads and response analysis of a monopile supported offshore wind turbine using fully coupled simulation[J]. *Renewable Energy*, 101, 126–143.
DOI: 10.1016/j.renene.2016.08.056

Sørensen NN, 1995. General purpose flow solver applied to flow over hills[J]. *Chinese Journal of Ship Research.*

Sørensen JN, Shen WZ, 1999. Computation of Wind Turbine Wakes using Combined Navier-Stokes/Actuator-line Methodology[J]. *Proceedings of European Wind Energy Conference EWEC* '99, 56-159, Nice.

So□rensen JN, Shen WZ, 2002. Numerical modeling of wind turbine wakes. *Journal of fluids engineering*, 124(2), 393-399.
DOI: 10.1115/1.1471361

Troldborg N, 2008. *Actuator Line Modeling of Wind Turbine Wakes*. Ph.D. Thesis, Department of Fluid Mechanics, Technical University of Denmark, Lyngby, Denmark.

Troldborg N, Larsen GC, Madsen HA, et al, 2011. Numerical simulations of wake interaction between two wind turbines at various inflow conditions[J]. *Wind Energy*, 14(7):859-876.
DOI: 10.1002/we.433

Vermeer LJ, Sørensen JN, Crespo AS, 2003. Wind turbine wake aerodynamics. Prog Aerosp Sci[J]. *Progress in Aerospace Sciences*, 39(6):467-510.
DOI: 10.1016/S0376-0421(03)00078-2

Wilmar H, Luis LPJ, Maldonado-Correa JL, 2016. Power Performance Verification of a Wind Farm Using the Friedman's Test[J]. Sensors, 16(6):816.
DOI:10.3390/s16060816

Zhao W, Shen Z, Wan D, 2014. Numerical investigation of the Vortex Induced Motion of SPAR in uniform current[M]// Magnetic Coupling between the Interior and Atmosphere of the Sun. Springer Berlin Heidelberg, 518-519.